Pharmacological Research - Modern Chinese Medicine 9 (2023) 100303

Contents lists available at ScienceDirect

Pharmacological Research - Modern Chinese Medicine

journal homepage: www.elsevier.com/locate/prmcm

Exploring the *in vitro* and *in vivo* anticancer activity of lasiokaurin on nasopharyngeal carcinoma

Huanhuan Pu [a,b], Jinrong Lin [a], Li-Sha Shen [c], Yu-Shan Lin [b], Rui-Hong Gong [d], Guo Qing Chen [b,d,e,*], Sibao Chen [a,b,d,e,*]

[a] *Institute of Medicinal Plant Development, Chinese Academy of Medical Sciences and Peking Union Medical College, Beijing 100193, China*
[b] *State Key Laboratory of Chinese Medicine and Molecular Pharmacology (Incubation), The Hong Kong Polytechnic University Shenzhen Research Institute, Shenzhen 518057, China*
[c] *Chongqing Academy of Chinese Materia Medica, Chongqing 400065, China*
[d] *Department of Food Science and Nutrition, The Hong Kong Polytechnic University, Hung Hom, Hong Kong 999077, China*
[e] *Research Centre for Chinese Medicine Innovation, The Hong Kong Polytechnic University, Hung Hom, Hong Kong 999077, China*

ARTICLE INFO

Keywords:
Lasiokaurin
Nasopharyngeal carcinoma
Apoptosis
Cell cycle arrest
Migration
Invasion

ABSTRACT

Objective: To evaluate the anticancer activity of the natural diterpenoid lasiokaurin (LAS) against nasopharyngeal carcinoma (NPC) both *in vitro* and *in vivo*, along with investigating its underlying mechanism.
Methods: MTT and colony formation assays were used to assess cell viability. Flow cytometry was utilized for the analysis of cell cycle arrest and apoptosis. Additionally, wound healing and transwell invasion assays were conducted separately to investigate cell migration and invasion. To uncover potential targets and pathways of LAS within NPC, a network pharmacological study based on RNA-sequencing (RNA-seq) was performed. Immunoblotting was subsequently used to determine protein levels. Furthermore, the anti-NPC activity of LAS was evaluated *in vivo* using a xenograft mouse model.
Results: Based on *in vitro* investigations, it is evident that LAS exerted substantial inhibitory effects on NPC cells. Notably, LAS demonstrated significant reductions in cell viability, migration, and invasion capabilities, while simultaneously inducing apoptosis and G2/M cell cycle arrest. Furthermore, LAS suppressed the activation of MAPK, mTOR, STAT3, and NF-κB pathways within NPC cells. Additionally, *in vivo* experiments underscored LAS's capacity to attenuate NPC tumor growth without eliciting any discernible impact on body weight.
Conclusion: Our data clearly demonstrate the anticancer activity of LAS against NPC, both *in vitro* and *in vivo*. These findings firmly position LAS as a potential candidate for the treatment of NPC.

Introduction

Nasopharyngeal carcinoma (NPC), a malignant head and neck tumor, exhibits notable regional and ethnic variations, frequently manifesting in southern China and Southeast Asia[1]. The International Agency for Research on Cancer (IARC) estimated 133,354 cases of NPC in 2020, accounting for 0.7% of all cancers and a mortality rate of 0.8%, with over 60,000 occurrences in China alone [2]. Diagnosed primarily in its clinical moderate-advanced stage due to its deep-seated location and inconspicuous early symptoms, approximately 70% of NPC patients face advanced disease upon diagnosis [3]. While early NPC is conventionally managed with radiotherapy [4], this approach encounters limitations, often leading to recurrence and distant metastases [5]. Moreover, advanced and recurrent metastatic NPC frequently culminate in fatalities attributed to tumor invasion and metastasis [6]. The burgeoning investigations into natural products, benefiting from their diverse chemical compositions and plentiful availability, have gained momentum in the development of novel anticancer agents [7].

Lasiokaurin (LAS), shown in Fig. 1A, emerges as a natural diterpenoid derived from Isodon serra (Maxim.) Kudo, a notable traditional Chinese medicine known as "Xihuangcao". This herb has gained popularity for its applications in the treatment of diverse conditions, including arthritis, enteritis, jaundice, hepatitis, and acute cholecystitis [8]. Within this herb, LAS stands as a significant constituent, renowned

* Corresponding authors at: State Key Laboratory of Chinese Medicine and Molecular Pharmacology (Incubation), The Hong Kong Polytechnic University Shenzhen Research Institute, Shenzhen 518057, China.
E-mail addresses: guoqing.chen@polyu.edu.hk (G.Q. Chen), sibao.chen@polyu.edu.hk (S. Chen).

https://doi.org/10.1016/j.prmcm.2023.100303
Received 9 July 2023; Received in revised form 30 August 2023; Accepted 31 August 2023
Available online 7 September 2023

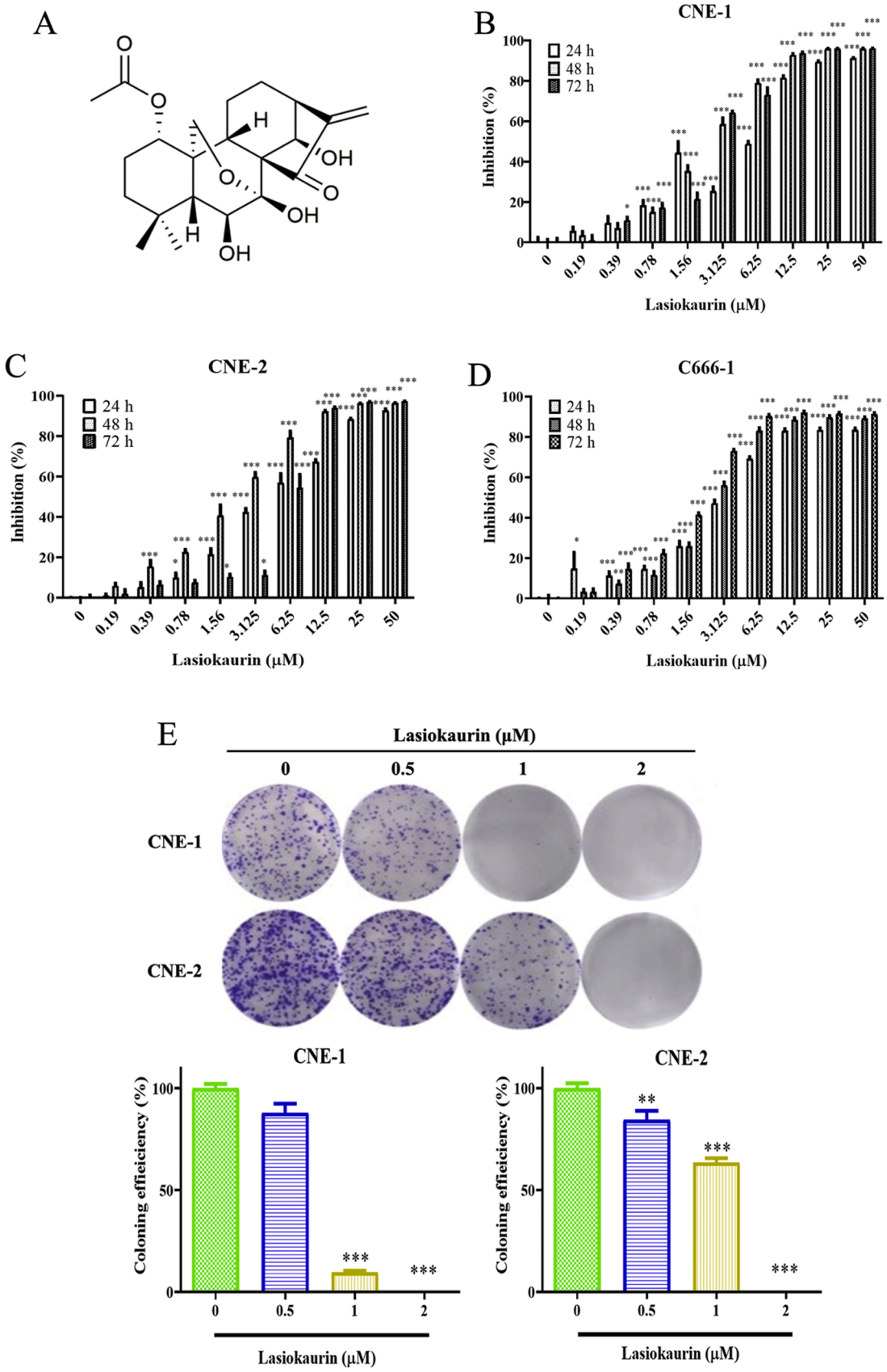

Fig. 1. LAS inhibited cell viability and colony formation in NPC cells. (**A**) Chemical structure of lasiokaurin. Cell viability of (**B**) CNE-1, (**C**) CNE-2, and (**D**) C666–1 was measured by MTT assay after LAS treatment at the indicated concentrations for 24, 48, and 72 h. (**E**) Colony formation of CNE-1 and CNE-2 cells treated with the indicated concentrations of LAS for 7 days. Data are shown as the means ± SD. $^{*}p < 0.05$, $^{**}p < 0.01$, $^{***}p < 0.001$ vs. control.

for its antimicrobial and anti-inflammatory activities [9,10]. Moreover, LAS has demonstrated anticancer potential across a spectrum of malignancies, encompassing gastric cancer, glioblastoma, hepatocarcinoma, lung adenocarcinoma, promyelocytic leukemia, and Ehrlich ascites carcinoma [11–14]. Notably, despite these findings, the extent of LAS's anticancer efficacy against NPC remains an unexplored territory, according to our current understanding.

This study aimed to explore the effectiveness of LAS against NPC both *in vitro* and *in vivo*, while investigating its underlying mechanisms. Notably, LAS exhibited a multifaceted impact on NPC cells, encompassing the inhibition of proliferation, migration, invasion, as well as the induction of cell cycle arrest and apoptosis. Additionally, LAS inhibited the activity of diverse pathways, including MAPK, mTOR, STAT3 and NF-κB. Furthermore, the anti-NPC potential of LAS was affirmed through its ability to impede tumor growth within a xenograft mouse model.

Materials and methods

Compounds

LAS ($C_{22}H_{30}O_7$; cat. no. CAS28957–08–6) was purchased from Jiangsu Yongjian Pharmaceutical Co., Ltd. (Jiangsu, China). The purity of LAS was > 98% as analyzed by high-performance liquid chromatography.

Cell culture

Human NPC cells CNE-1, CNE-2, and C666–1 were supplied by the Hong Kong NPC AoE Cell Line Repository and maintained in Dulbecco's Modified Eagle's Medium (DMEM) supplemented with 10% FBS and 1% Penicillin/Streptomycin at 37 °C in a humidified atmosphere containing 5% CO_2 and 95% air.

Cell viability assay

According to previous studies [15], cells were seeded for 24 h at a density of 4000 cells / well (CNE-1 and CNE-2) or 1×10^4 cells / well (C666–1) in 96-well plates, and then treated with various concentrations of LAS for 24, 48, or 72 h (0–50 μM). 20 μL MTT (2.5 mg/mL) was added to the medium in each well and incubated for 4 h at 37 °C. After discarding culture media, DMSO was added into the wells to dissolve the formed formazan, and the optical density values were measured at 570 nm through a Biotek Synergy H1 microplate reader (BioTek Instruments, Inc.).

Colony formation assay

CNE-1 and CNE-2 cells were seeded in triplicate at a density of 900 cells / well in 60-mm dishes with various concentrations of LAS for 7 days. At the end of the experiment, cells were fixed with 4% paraformaldehyde for 20 min, stained with Crystal Violet Staining Solution (Shanghai, China) 30 min, and rinsed with ultrapure water before imaging for quantification [16]. Colony counts were quantified using ImageJ software (Version 1.4.3.67, NIH, Bethesda, MD, USA).

Cell cycle analysis

Cell cycle distribution was assessed using the Cell Cycle and Apoptosis Analysis kit (Beyotime Biotechnology). CNE-1 and CNE-2 cells were seeded overnight at 3×10^5 cells / well in 60-mm dishes. After treated with LAS for 24 or 48 h, cells were harvested. Subsequently, cells were fixed with ice-cold 70% ethanol at −20 °C overnight, then rinsed with ice-cold PBS and incubated with propidium iodide (PI) for 30 min at 37 °C in the dark [17]. Flow cytometric cell analysis was performed using a BD FACSCalibur™ Flow Cytometry (BD Biosciences, San Jose, CA, USA) and the results were analyzed using ModFit LT 5.0 (Verity Software House, ME, USA).

Annexin V-FITC apoptosis assay

Cell apoptosis assay was assessed using the Annexin V-FITC Apoptosis Detection kit (Beyotime Biotechnology) [18]. CNE-1 and CNE-2 cells were seeded in 60-mm dishes were treated with LAS and then collected after 24 h. NPC cells were incubated with Annexin V-FITC and PI at room temperature for 20 min in the dark, subsequently placed on ice in the dark, and immediately assessed using a BD FACSAria™ IIflow cytometer (BD Biosciences, San Jose, CA, USA).

Wound healing assay

The migration ability of NPC was evaluated by wound-healing assays, as previously described [19]. CNE-1 and CNE-2 cells at a density of 3×10^4 cells / well were seeded into both chambers of the culture insert (ibidi, Germany). After cells attached overnight, the inserts were removed to create a wound. Subsequently, cells were treated with LAS in serum free medium, and images of the migrated cells were obtained under a microscope at 0, 12, 24, 36, and 48 h. Wound areas were quantified using ImageJ software. The relative wound healing rate was calculated as follows: relative wound healing rate (%) = (remaining wound area-original wound area vehicle) / original wound area vehicle × 100%.

Transwell invasion assay

Transwell invasion assay was performed using transwell polycarbonate membrane filter inserts (Corning Costar, USA) [20]. Briefly, CNE-1 cells at a density of 5×10^4 cells / well in serum free medium were seeded into upper chamber (8 μm pore size) for migration assay, or into upper chambers coated with matrigel for the invasion assay. Migration and invasion cultural periods were 24 h with LAS placed in the lower chamber, in complete medium with 10% FBS. After 24 h incubation at 37 °C, the remaining cells on the upper surface of the filter were removed using a cotton swab. Cells that invaded to the lower surface of the filter were fixed with 4% paraformaldehyde for 15 min, stained with Crystal Violet staining solution, rinsed with ultrapure water and counted under a light microscope.

Network pharmacological study

CNE-1 cells treated with or without LAS were lysed in Trizol. The global gene expression profiles were examined by RNA-seq in Novogene (Beijing, China). DESeq2_1.20.0 software was used for differential expression analysis between the two groups. Genes with an p-value < 0.05 and | log2(FoldChange) | ≥ 1 were assigned as differentially expressed genes. Then, the Gene Ontology (GO) and Kyoto Encyclopedia of Genes and Genomes (KEGG) processes were analyzed using the OmicsBean (http://www.omicsbean.cn/) and Metascape databases (http://metascape.org/gp/index.html) [21]. Finally, these targeted genes were validation by RT-PCR analysis. The information of primers in RT-PCR were shown in **Table S1**.

Western blot analysis

Following treated with different concentrations of LAS for 24 h, cells were harvested for western blot analysis according to the report [15]. Ice-cold RIPA buffer (Beverly, MA, USA) with PMSF (Sigma, MO, USA), protease inhibitor (Roche, Basel, Switzerland) and phosphatase inhibitor (Roche, Basel, Switzerland) were used for cell lysis. Protein concentrations were determined by Pierce™ BCA Protein Assay (Waltham, MA, USA). Protein samples (15 μg / well) were separated by SDS-PAGE in polyacrylamide gels followed by transfer to PVDF membranes.

Subsequently, membranes were blocked in 5% non-fat skim milk diluted in TBST and incubated with primary antibodies (1:1000) in 5% BSA diluted in TBST overnight at 4 °C. After washing with TBST buffer, membranes were incubated with corresponding secondary antibodies (1:5000). The primary antibodies used were the following: p-STAT3 (ab76315), STAT3 (ab68153), p-mTOR (ab137133), mTOR (ab2732), Raptor (ab26264), Rictor (ab70374), Gβl (ab228832), p-NF-κB (ab86299), NF-κB (ab16502), p-p38(ab195049), p38 (ab170099), p-Erk1/2(ab176660), Erk1/2 (ab54230), Bax (ab216494), cyclin B1 (ab215436), cdc2 (ab133327), MMP-9 (ab76003, all from Abcam, 1:1000 dilution) and β-actin (ZSGB-Bio, 1:5000 dilution).

Mouse xenograft tumor model

6-week-old male BALB/c nude mice were purchased from Speyford (Beijing, China) Biotechnology Co., Ltd. and were housed in a specific pathogen free (SPF)-grade animal facility with free access to food and water. All animal experiments were approved by the Chinese Academy of Medical Sciences and Peking Union Medical College Animal Subjects Ethics Subcommittee and conducted in accordance with the Institutional Guidelines and Animal Ordinance of the Department of Health. Mice were inoculated with 2×10^6 CNE-2 cells suspended in 0.1 ml DMEM without FBS in the right armpit as previously reported [15]. When the average tumor volume reached 100 mm^3 on the 12 days, mice were randomly divided into three groups ($n = 5$ mice / group). The treatment groups were as follows: Mice in the vehicle group were injected intraperitoneally daily with equivalent amount of solvent (5% Cremophor EL and 5% ethanol in saline; 10 ml/kg). Mice in the LAS group were injected intraperitoneally daily with 10 [LAS-Low Dose (LD)] or 20 mg/kg [LAS-High Dose (HD)] LAS. The body weights and tumor sizes were measured every 2 days. Tumor volumes were calculated using the formula ($L \times W^2$)/ 2 mm^3 (L = length; W= width). All mice were euthanized by CO_2 inhalation on 12 days, and their tumors were harvested and weighed. Tumors were fixed in 4% paraformaldehyde and embedded with paraffin. The next, paraffin-embedded tumors were cut into 4 μm sections, following by staining with hematoxylin and eosin (H&E) and Ki67 antibody (Servicebio, Wuhan, China). Stained sections were pictured using a Nikon microscope.

Statistical analysis

All data were expressed as means ± S.E.M., statistical differences between groups were analyzed by one-way analysis of variance (ANOVA). $^*p < 0.05$, $^{**}p < 0.01$, $^{***}p < 0.001$ vs. control.

Results

LAS inhibits the proliferation of NPC cells

To assess the anticancer activity of LAS against NPC, we employed three NPC cell lines (CNE-1, CNE-2, and C666–1) for our study. Initially, we investigated the inhibitory effect of LAS on the proliferation of NPC cells. The results of the MTT assay demonstrated a significant dose- and time-dependent reduction in the viability of all three NPC cell lines due to LAS treatment (Fig. 1B-D). To further evaluate the long-term inhibitory effects, we conducted a colony formation assay specifically on CNE-1 and CNE-2 cells. The results, shown in Fig. 1E and Table. S2, highlighted the substantial reduction in colony formation ability, even when exposed to a low LAS concentration. These collective findings indicate that LAS effectively inhibits the proliferation of NPC cells *in vitro*.

LAS induces cell cycle G2/M arrest in NPC cells

Given the well-established link between cell cycle progression and cell proliferation [22], our investigation focused on the impact of LAS treatment on the cell cycle distribution of CNE-1 and CNE-2 cells. Notably, as time and concentration increased, the proportion of NPC cells in the G2/M phase displayed a significant rise (Fig. 2A,B). This observation strongly implies that LAS administration leads to a dose- and time-dependent arrest of NPC cells in the G2/M phase of the cell cycle. To further determine the role of LAS in cell cycle regulation, we evaluated the levels of cyclin B1 and cdc2, both crucial checkpoints within the G2/M phase. Our findings revealed a decrease in the expression of cyclin B1 and cdc2 in both CNE-1 and CNE-2 cells upon LAS treatment (Fig. 2C-F). These results collectively underscore LAS's effect on the G2/M cell cycle arrest.

LAS induces apoptosis in NPC cells

Alongside cell cycle regulation, the induction of apoptosis stands as a vital avenue in cancer treatment strategies [23]. To investigate LAS's effect on inducing apoptosis in NPC cells, we employed Annexin V-FITC/PI staining with flow cytometry [24]. The results, as shown in Fig. 3A, exhibited a noticeable increase in the percentage of apoptotic cells corresponding to escalating LAS concentrations. Subsequently, we conducted western blot analyses on LAS-treated CNE-1 and CNE-2 cells to measure the expression of Bax, a pivotal apoptotic marker [25,26]. The results in Fig. 3B-E demonstrated a significant increase in Bax expression upon LAS treatment, thus confirming LAS's role in inducing apoptosis in NPC cells.

LAS inhibits the migration and invasion of NPC cells

Given the notably high metastatic rate associated with NPC [27], an imperative aspect of assessing potential treatments is the evaluation of their anti-metastatic properties. Moreover, considering the established efficacy of apoptosis induction in inhibiting cancer cell metastasis [28], and taking into account the outcomes illustrating LAS's capacity to trigger apoptosis in NPC cells, we subsequently undertook examinations of LAS's anti-metastatic potential on NPC cells. We employed distinct wound healing and transwell invasion assays to find out the extent to which LAS impacts the migration and invasion capabilities of NPC cells. The results, depicted in Fig. 4A-D, unveiled a substantial reduction in the wound healing rates of LAS-treated CNE-1 and CNE-2 cells. This observation serves as a clear indication of LAS's effective dose- and time-dependent inhibition of migration. Similarly, the invasion ability of both CNE-1 and CNE-2 cells was dose-dependently inhibited by LAS, as shown in Fig. 5A-C. Furthermore, we conducted western blot assay on LAS-treated CNE-1 and CNE-2 cells to analyze the expression of MMP-9, an established molecular biomarker for NPC metastasis [29,30]. As shown in Fig. 5D-G, LAS effectively diminished MMP-9 expression in both CNE-1 and CNE-2 cells, thereby confirming its ability to inhibit NPC metastasis.

Screening potential targets and pathways of LAS in NPC

To discern potential molecular mechanisms underlying LAS's efficacy in NPC treatment, we conducted a network pharmacological study utilizing RNA-sequencing (RNA-seq). Specifically, CNE-1 cells were exposed to LAS (5 μM), and subsequent RNA-seq analysis was performed. Differential gene expression analysis was then employed to identify genes exhibiting altered expression between the LAS-treated and control groups. The results, as shown in Fig. 6A, unveiled 719 differentially expressed genes (DEGs) in LAS-treated cells *versus* untreated counterparts. Among these, 428 genes experienced upregulation (indicated in blue), while 291 genes displayed downregulation (depicted in gray). To further validate the RNA-seq findings, we subjected 17 of these genes to RT-PCR analysis. This verification confirmed the downregulation of mRNA expression in JUND, CD70, KRT15, KRT19, and TAF15 (Fig. 6B), and the upregulation of AREG, DUSP4, EPHA2, TGFA, GADD45A, VEGFA, CDKN1A, GDF15, LAMB3, FN1, PLAU, and FOSL1 (Fig. 6C)—consistent with the RNA-seq data. GO

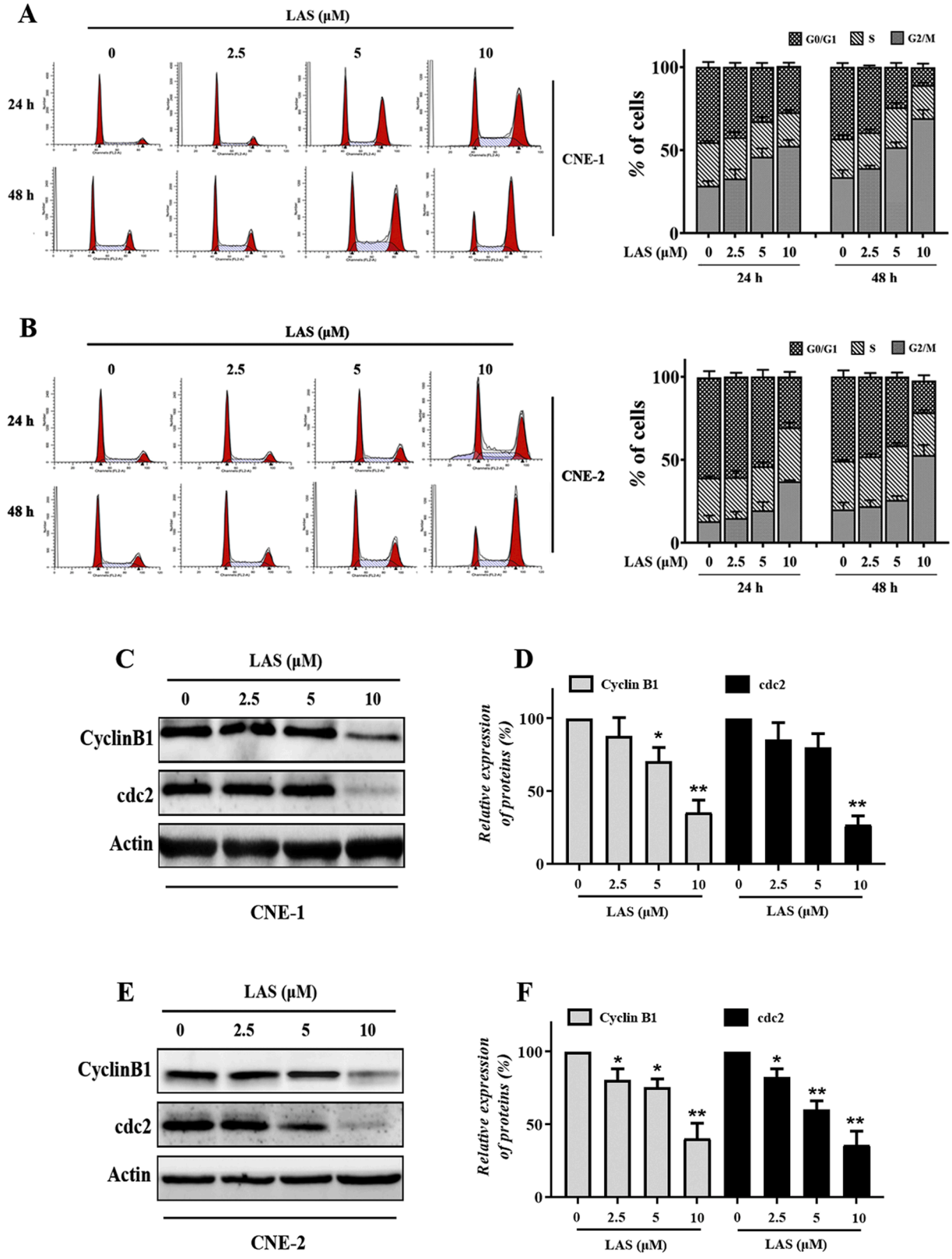

Fig. 2. LAS induced cell cycle arrest at the G2/M phase in NPC cells. (**A**) Flow cytometry (left panel) and histogram (right panel) analyses of CNE-1 cells treated with LAS for 24 or 48 h, respectively. (**B**) Flow cytometry (left panel) and histogram (right panel) analyses of CNE-2 cells treated with LAS for 24 or 48 h, respectively. (**C**) Western blot (left panel) and (**D**) histogram (right panel) of the expression of Cyclin B1 and cdc2 in CNE-1 cells treated LAS for 24 h. $^{*}P < 0.05$, $^{**}P < 0.01$, compared with control group. (**E**) Western blot (left panel) and (**F**) histogram (right panel) of the expression of Cyclin B1 and cdc2 in CNE-2 cells treated LAS for 24 h. $^{*}P < 0.05$, $^{**}P < 0.01$, compared with control group.

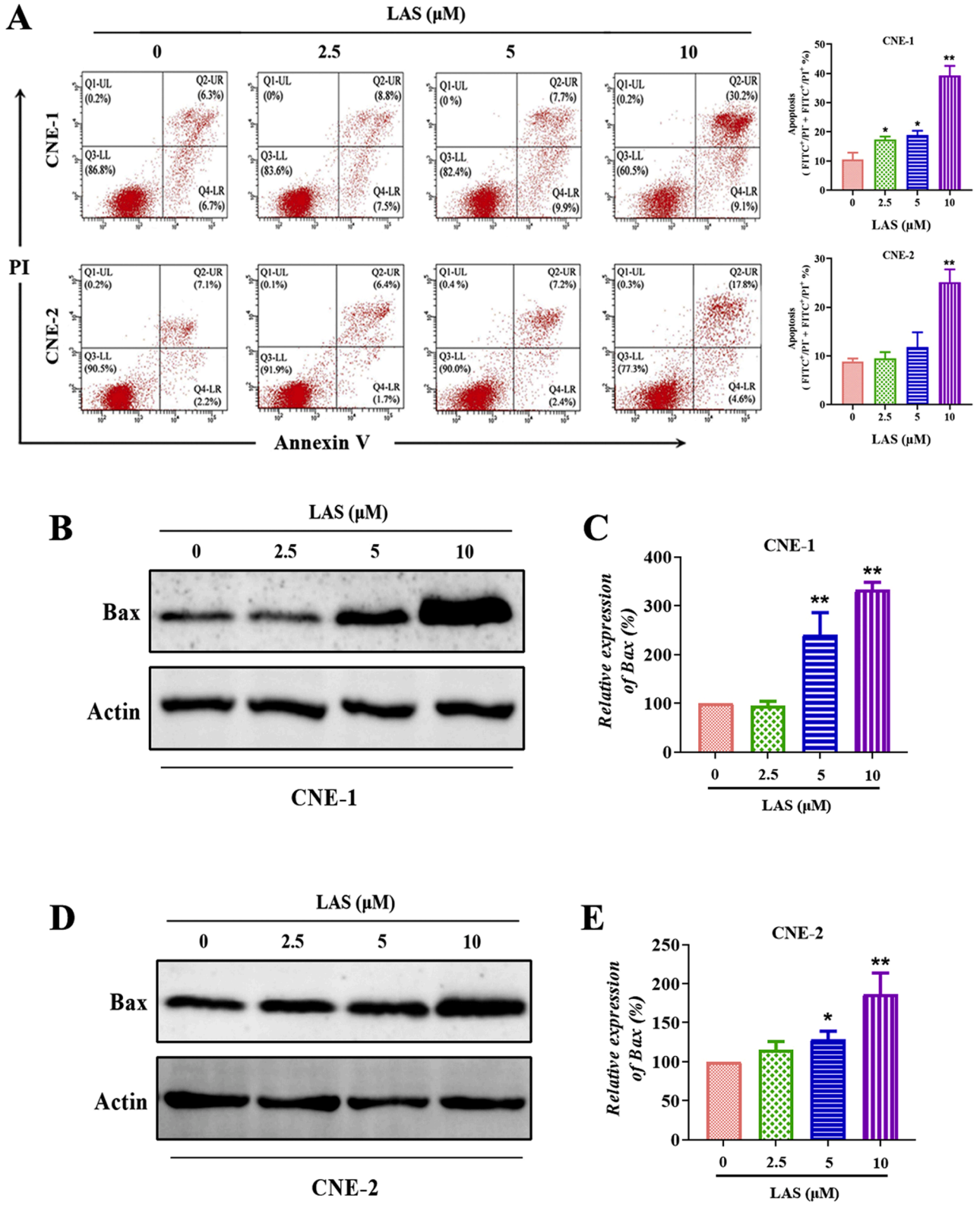

Fig. 3. LAS induced apoptosis in NPC cells. (**A**) Flow cytometry (left panel) and histogram (right panel) analyses of CNE-1 and CNE-2 cells treated with LAS for 24 or 48 h, respectively. Cells in Q1-UL were stained for $FITC^{-}/PI^{+}$, which indicates necrosis; Cells in Q2-UR were stained for $FITC^{+}/PI^{+}$, which indicates late apoptosis; Cells in Q3-LL were stained for $FITC^{-}/PI^{-}$, which indicates survive; Cells in Q4-LR were stained for $FITC^{+}/PI^{-}$, which indicates early apoptosis. (**B**) Protein expression of Bax and (**C**) quantitative analysis of Bax in CNE-1 cells treated with LAS for 24 h, $^{**}P < 0.01$. (**D**) Protein expression of Bax and (**E**) quantitative analysis of Bax in CNE-2 cells treated with LAS for 24 h, $^{*}P < 0.05$, $^{**}P < 0.01$.

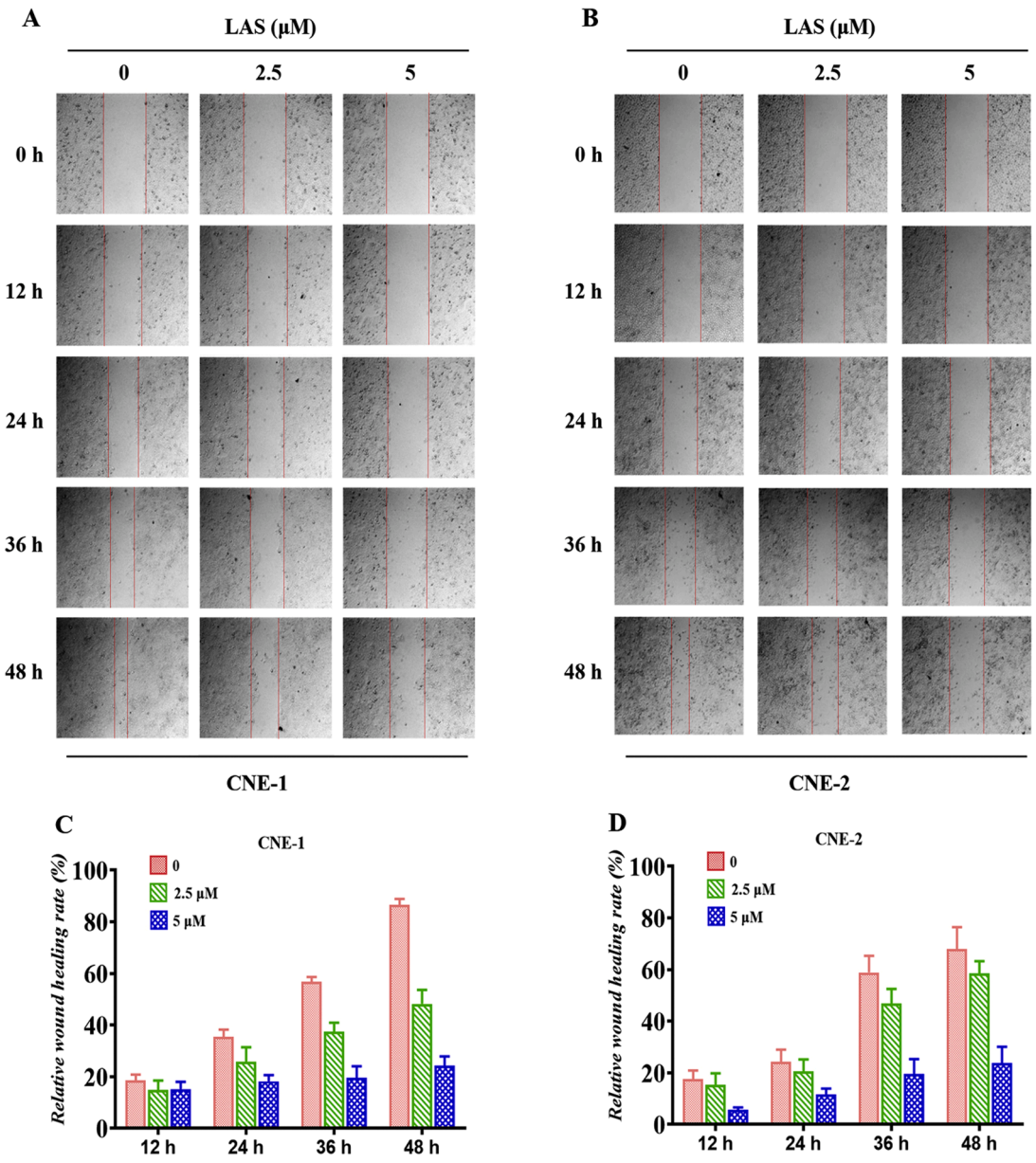

Fig. 4. LAS inhibited the migration of NPC cells. (**A**) LAS reduced the wound healing of CNE-1 cells. (**B**) LAS reduced the wound healing of CNE-2 cells. (**C**) Quantitative analysis of relative wound healing rates in CNE-1. (**D**) Quantitative analysis of relative wound healing rates in CNE-2.

enrichment analysis, as shown in Fig. 6D, delineated the top 10 significant GO terms. Notably, cellular component analysis unveiled marked differences in categories such as extracellular region, extracellular matrix, and extracellular region part ($p < 0.05$, Table. S3). KEGG analysis further determined 20 key signaling pathways linked to LAS's anticancer effects in NPC cells, encompassing pathways such as MAPK and PI3K-Akt (Fig. 6E). Additionally, the genes presented in Figure. S1 and S2, linked to these pathways, were in agreement with the previously identified DEGs data.

LAS inhibits the MAPK pathway in NPC cells

The activation of the MARK pathway is recognized for its role in promoting NPC tumor growth, cell invasion and metastasis [31,32]. Previous DNA-seq data indicated a potential link between this pathway and LAS's anti-NPC activity, prompting our investigation into LAS's impact on MAPK pathway regulation. As shown in Fig. 7A,B, the phosphorylation levels of Erk1/2 and p38 underwent a marked reduction in LAS-treated CNE-1 and CNE-2 cells.

LAS inhibits the mTOR and STAT3 pathways in NPC cells

Considering prior RNA-seq data suggesting an association between the PI3K-Akt pathway and LAS's effects in NPC cells, we extended our analysis to mTOR expression, an essential node within this pathway, critical for cell survival, proliferation, and metabolism [33,34]. As shown in Fig. 7C,D, the phosphorylation levels of mTOR displayed a significant reduction in LAS-treated CNE-1 and CNE-2 cells. Moreover, we explored the expression levels of STAT3, another pivotal factor influencing NPC cell proliferation, invasion, and migration [35], along with the expression of p-STAT3. These expressions exhibited a consistent, dose-dependent decrease upon LAS treatment (Fig. 7C,D). The mTOR pathway encompasses two distinct multiprotein complexes (mTORC1 and mTORC2), both integral to the PI3K/Akt pathway [36]. To determine the specific complex targeted by LAS's anticancer activity in NPC, we examined Rictor, Raptor, and Gβl expression levels. Raptor

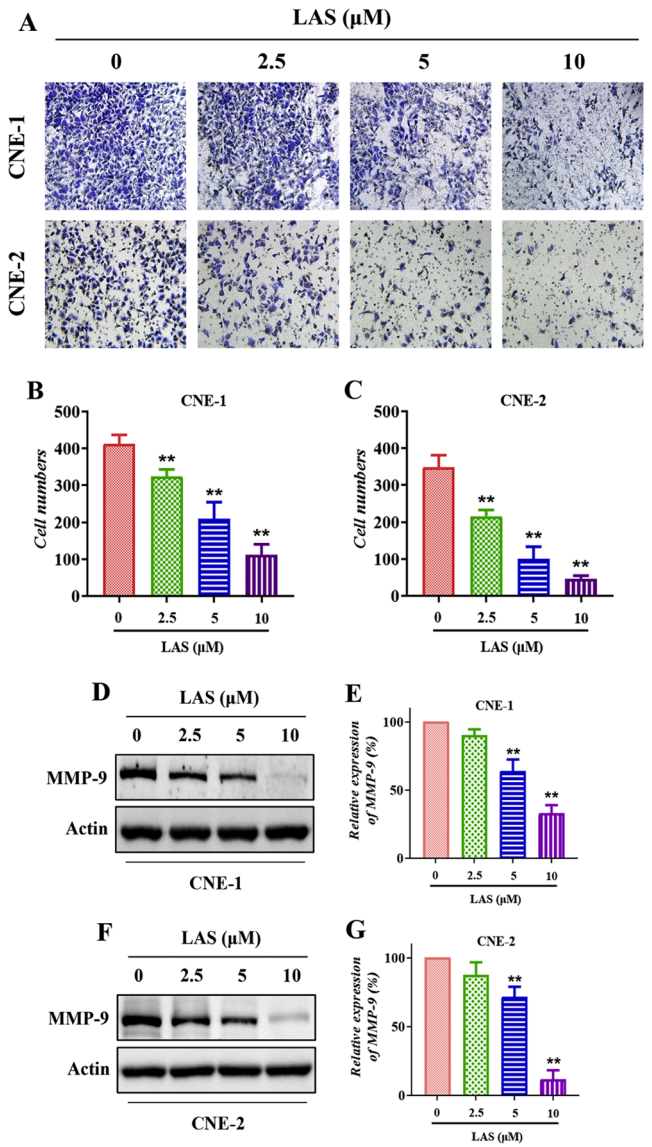

Fig. 5. LAS inhibited the invasion of NPC cells. (**A**) CNE-1 and CNE-2 cells invasion under LAS treatment of 24 h was assessed through transwell invasion assay. (**B**) The number of invasive CNE-1 cells was counted, $^{**}P < 0.01$. (**C**) The number of invasive CNE-2 cells was counted, $^{**}P < 0.01$. (**D**) Protein expression of MMP-9 and (**E**) quantitative analysis of MMP-9 in CNE-1 cells treated with LAS for 24 h, $^{**}P < 0.01$. (**F**) Protein expression of MMP-9 and (**G**) quantitative analysis of MMP-9 in CNE-2 cells treated with LAS for 24 h, $^{**}P < 0.01$.

and Rictor are subunits specific to mTORC1 and mTORC2, respectively; while Gβl is shared by both mTORC1 and mTORC2 [37]. The findings depicted in Fig. 7E,F illustrated reduced expression of these three components under LAS treatment, implying that LAS effectively inhibits both mTORC1 and mTORC2.

LAS inhibits the NF-κB pathway in NPC cells

Given the recognized connection between constitutive NF-κB pathway activation and NPC, particularly in Epstein-Barr virus (EBV)-positive cases [38], our investigation proceeded to explore the potential of LAS to suppress this pathway. As shown in Fig. 7G,H, LAS led to a significant reduction in the phosphorylation levels of NF-κB in both CNE-1 and CNE-2 cells.

LAS inhibits tumor growth in vivo

To assess the *in vivo* anticancer efficacy of LAS, a mouse xenograft model was established by inoculating CNE-2 cells into the right armpit. Subsequent to success of tumor inoculation, mice were subjected to daily intraperitoneal administration of LAS, either at 10 mg/kg (LD group) or 20 mg/kg (HD group), for a continuous 12-day period. The vehicle groups received corresponding intraperitoneal injections of saline. After the 12-day treatment, mice were sacrificed, and the xenograft tumors were excised for evaluation. As shown in Fig. 8A-C, both tumor volume and weight underwent a significant reduction in the LAS-LD and LAS-HD groups, providing compelling evidence of LAS's ability to inhibit NPC tumor growth. The changes in mice body weight during the administration period were shown in Fig. 8D. Remarkably, mice in both the LAS-LD and LAS-HD groups did not demonstrate the gradual weight gain that was observed in the vehicle group. Nonetheless, the body weight of mice in both LAS-HD and LAS-LD groups remained relatively stable throughout the administration period. Furthermore, the histopathological characteristics of the tumors were assessed. The outcomes depicted in Fig. 8E revealed dense cellular packing in the tumor samples from the vehicle group. In contrast, the tumor samples from the LAS-treated groups displayed numerous vacuoles, particularly prominent in the LAS-HD group. Additionally, a decreased presence of Ki67-positive cells, indicative of proliferative activity, was noted in the tumor samples from the LAS groups (Fig. 8E), thereby confirming LAS's inhibitory effect on NPC tumor growth.

Discussion

Endemic to southern China and southeast Asia, NPC is colloquially referred to as Guangdong Cancer due to its high incidence in these regions [39]. Epidemiological investigations have established the multifaceted etiology of NPC, linking it to Epstein-Barr virus (EBV) infection as well as environmental and genetic factors [40]. The gravity of the situation lies in NPC's association with substantial mortality and morbidity, underscoring the imperative to develop effective treatments [41]. In this context, natural products have garnered attention for their reported potential in the prevention and treatment of NPC, offering a promising avenue to mitigate the limitations of chemotherapy and its associated side effects [15,42].

LAS, a natural diterpenoid found in Isodon plants, has yet to receive significant attention within the research community. While some studies have acknowledged its potential anticancer properties, its specific anti-NPC activity and underlying mechanisms remain largely uncharted. This study seeks to address this gap by conducting an initial exploration into the effects of LAS on NPC.

We commenced by establishing LAS's inhibitory impact on NPC cell proliferation through MTT and colony formation assays. Considering the intricate interplay between cell cycle regulation and proliferation, we investigated the modulation of cell cycle progression by LAS [43]. Notably, our subsequent analyses revealed LAS's role in reducing the expression of cyclin B1 and cdc2, indicating its capacity to induce cell cycle G2/M arrest. Apoptosis represents a cancer treatment strategy embraced by various natural compounds [18]. This prompted us to analyze LAS-induced apoptosis within NPC cells through Annexin V-FITC/PI staining, which revealed a notable rise in the proportion of apoptotic cells. Moreover, our examination of NPC cells exposed to LAS showed an elevation in Bax expression, a compelling confirmation of LAS's apoptosis-inducing capabilities.

In clinical practice, the primary cause of mortality among NPC patients is often attributed to tumor recurrence and metastases [44]. Consequently, any potential anti-NPC candidates warrant consideration of their anti-metastatic properties. Moreover, given our observation of LAS's capacity to induce apoptosis, a pivotal mechanism in inhibiting metastasis [28], we proceeded to evaluate the possible inhibitory impact of LAS on NPC cell metastasis. Notably, LAS exhibited inhibitory effects

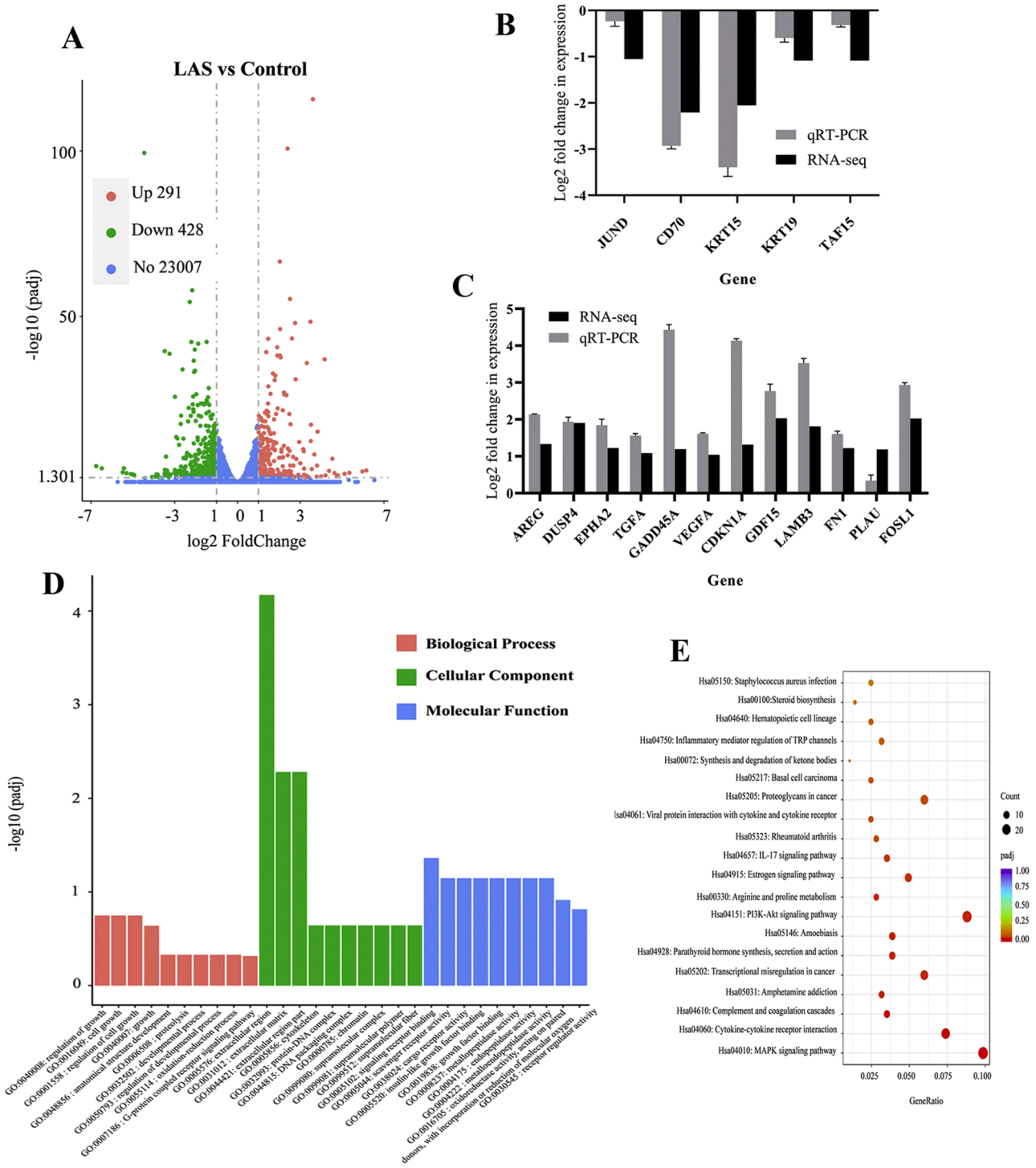

Fig. 6. Network pharmacological study on the effects of LAS based on RNA-seq data. (**A**) Volcano plots of differentially expressed genes (DEGs). DEGs with absolute fold change of 2 > 1 and *p*-value < 0.05 were shown. (**B**) Down-regulated genes and (**C**) up-regulated genes were analyzed through RT-PCR. (**D**) GO enrichment of related genes. (**E**) Top 20 pathways enriched by the KEGG method.

on both NPC cell migration, as demonstrated by wound-healing assays, and their invasion capacity, as assessed through transwell assays. Furthermore, we observed a reduction in MMP-9 expression in NPC cells treated with LAS, providing further confirmation of LAS's ability to inhibit NPC metastasis.

To uncover the potential underlying anticancer mechanism of LAS in NPC, we conducted a network pharmacological investigation based on RNA-seq data. This comprehensive analysis yielded a total of 719 DEGs distinguishing the LAS-treated and control groups. Further, the examination of key pathways revealed 20 associations integral to LAS's anti-NPC activity, prominently featuring pathways such as MAPK and PI3K-Akt. To validate the outcomes of our network pharmacological study, we proceeded to measure the expression of Erk1/2, p38, and mTOR through western blot analysis. Remarkably, these three factors demonstrated a reduction in phosphorylation following LAS treatment. This finding, in turn, underscored LAS's capability to suppress MAPK and PI3K-Akt activation. Continuing our exploration, we investigated the regulatory impact of LAS on the STAT3 and NF-κB pathways within

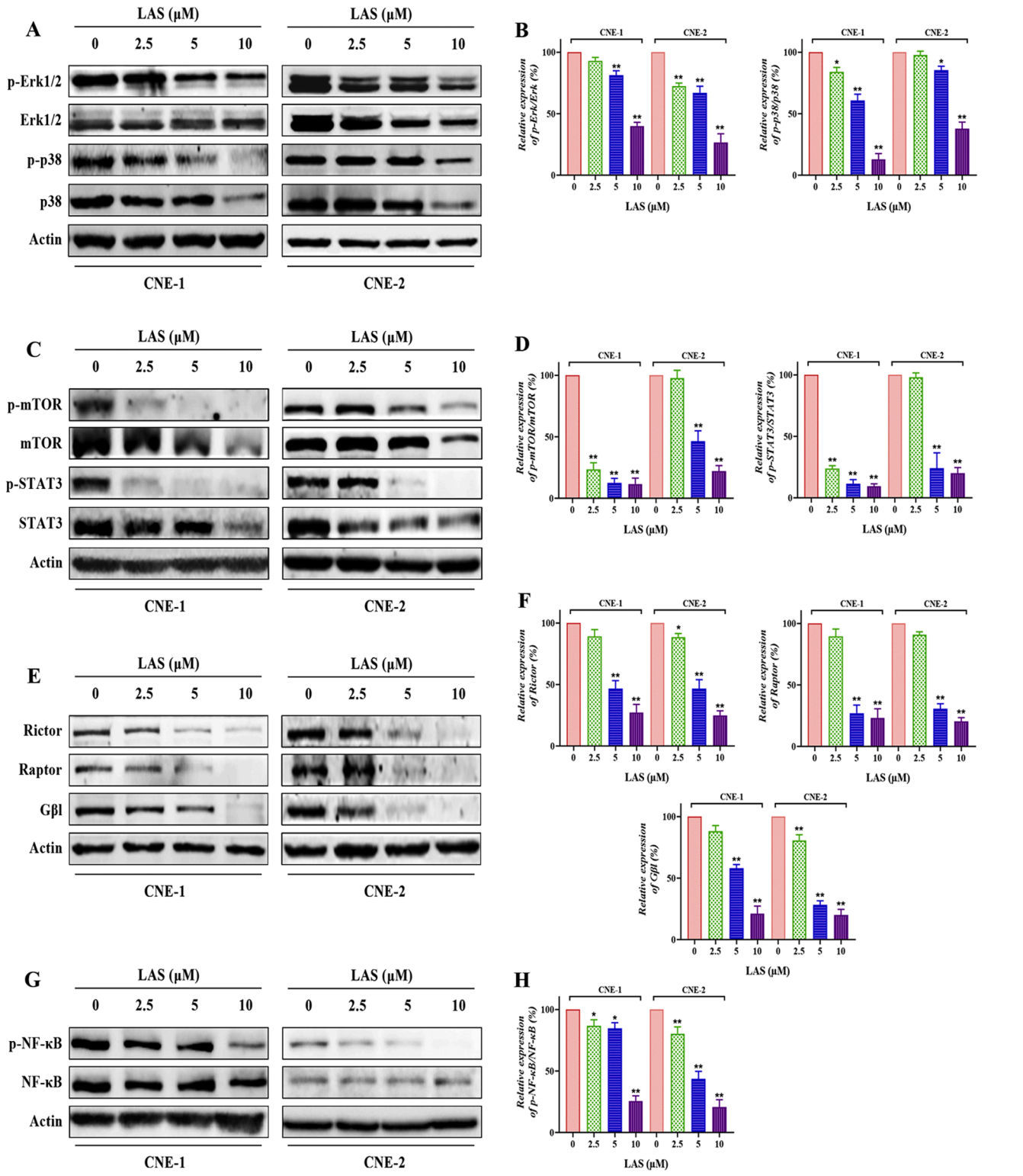

Fig. 7. LAS suppressed MAPK, mTOR, STAT3, and NF-κB pathways in NPC cells. (**A**) Protein expression, and (**B**) quantitative analysis of Erk1/2 and p38 in NPC cells treated with LAS for 24 h, $^{*}P < 0.05$, $^{**}P < 0.01$. (**C**) Protein expression, and (**D**) quantitative analysis of mTOR and STAT3 in NPC cells treated with LAS for 24 h, $^{*}P < 0.05$, $^{**}P < 0.01$. (**E**) Protein expression, and (**F**) quantitative analysis of Rictor, Raptor and Gβl in NPC cells treated with LAS for 24 h, $^{*}P < 0.05$, $^{**}P < 0.01$. (**G**) Protein expression, and (**H**) quantitative analysis of NF-κB in NPC cells treated with LAS for 24 h, $^{*}P < 0.05$, $^{**}P < 0.01$.

NPC cells. The results confirmed LAS's role in reducing the phosphorylation of these factors, thereby signifying its inhibitory influence on both STAT3 and NF-κB pathways.

Transitioning from *in vitro* investigations, we evaluated the inhibitory effects of LAS on tumor growth through an NPC subcutaneous xenograft mouse model. The *in vivo* study notably demonstrated that LAS at a dosage of 20 mg/kg exhibited a significant capacity to inhibit tumor growth. While the body weight of mice in the two LAS groups did not show the same gradual increase as observed in the vehicle group, there was no significant change in the body weight of mice in both

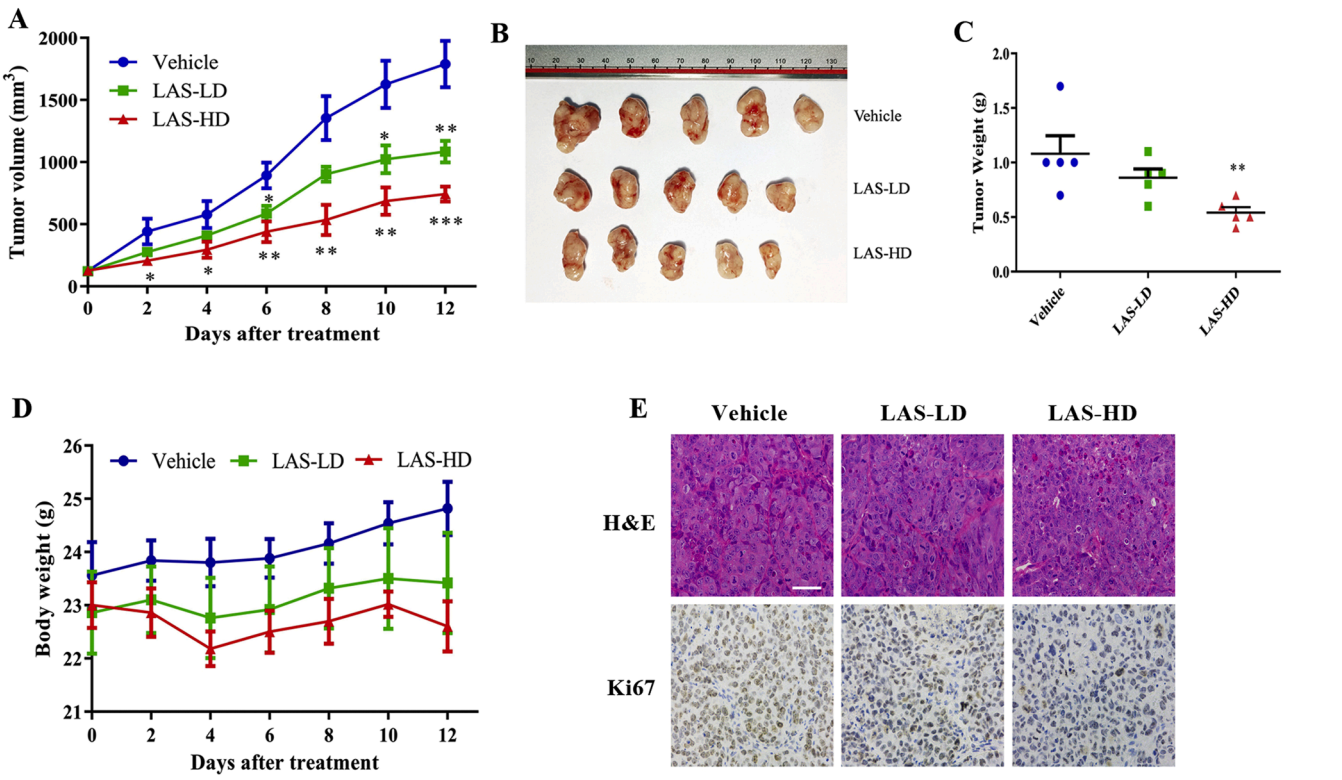

Fig. 8. LAS inhibited *in vivo* CNE-2 xenograft tumor growth. A xenograft model was established by subcutaneous inoculation of CNE-2 cells into BALB/c nude mice. When the average tumor volumes reach to 100 mm^3, mice were randomly divided into three groups and daily administrated with vehicle (5% of Cremophor EL, 5% of ethanol in saline), LAS-LD (10 mg/kg), or LAS-HD (20 mg/kg) daily via i.p. injection. The treatment period lasted for 12 days and all mice were sacrificed. (**A**) Tumor volumes were measured throughout the experimental period, $^*p < 0.05$, $^{**}p < 0.01$, $^{***}p < 0.001$ vs. control. (**B**) Images of tumors at the end of experiment. (**C**) Tumor weights at experimental endpoint. (**D**) Mouse body weights throughout the experimental period. (**E**) Tumors were stained with H&E and Ki67. Scale bar = 100 μm.

groups before and after administration, indicating that LAS may be safe.

Limitations

This study has some limitations. Owing to constraints in financial resources and time, we encountered limitations in conducting more in-depth mechanism and safety studies.

This included the task of pinpointing the specific protein targets of LAS within NPC cells, understanding its metabolism, and assessing its distribution within living tissues. Addressing these issues requires future research efforts aimed at expanding our understanding.

Conclusions

In summary, our studies have unveiled a multifaceted impact of LAS on NPC cells. Notably, LAS has demonstrated the ability to inhibit NPC cell proliferation, induce G2/M cell cycle arrest and apoptosis, and suppress cell migration and invasion. Furthermore, we conducted a comprehensive analysis of gene expression patterns within LAS-treated CNE-1 cells using RNA-seq technology. Subsequently, LAS's inhibitory effects extend to pivotal pathways such as MAPK, mTOR, NF-κB, and STAT3 within NPC cells. These observations collectively underscore LAS's broad-reaching influence across multiple molecular pathways. Moreover, our findings extend into the *in vivo* context, with LAS showing its significant potential by substantially inhibiting tumor growth. These findings not only enhance our comprehension of LAS's efficacy against NPC but also introduce novel perspectives for the future development of LAS as a prospective therapeutic agent for treating NPC.

Institutional review board statement

All animal experimental procedures were performed according to the Institutional Guidelines and Animal Ordinance of the Department of Health, and approved by the Chinese Academy of Medical Sciences and Peking Union Medical College Animal Subjects Ethics Subcommittee (SLXD-20211101013, 1 November 2021).

Declaration of Competing Interest

The authors declare that they have no known competing financial interests or personal relationships that could have appeared to influence the work reported in this paper.

Formatting of funding sources

This study was supported by the Hong Kong Polytechnic University Start-up Fund (P0036741 and P0038596), the National Natural Science Foundation of China (No. 81872769), Chongqing Science and Technology Commission (JA21026), Shenzhen Science and Technology Innovation Commission (JCYJ20220531090802006).

Supplementary materials

Supplementary material associated with this article can be found, in the online version, at doi:10.1016/j.prmcm.2023.100303.

References

[1] J. Chou, Y.C. Lin, J. Kim, L. You, Z. Xu, B. He, D.M. Jablons, Nasopharyngeal carcinoma–review of the molecular mechanisms of tumorigenesis, Head Neck 30 (7) (2008) 946–963.

[2] H. Sung, J. Ferlay, R.L. Siegel, M. Laversanne, I. Soerjomataram, A. Jemal, F. Bray, Global cancer statistics 2020: GLOBOCAN estimates of incidence and mortality worldwide for 36 cancers in 185 countries, CA Cancer J. Clin. 71 (3) (2021) 209–249.

[3] B. Zhang, M.M. Li, W.H. Chen, J.F. Zhao, W.Q. Chen, Y.H. Dong, X. Gong, Q. Y. Chen, L. Zhang, X.K. Mo, X.N. Luo, J. Tian, S.X. Zhang, Association of chemoradiotherapy regimens and survival among patients with nasopharyngeal carcinoma: a systematic review and meta-analysis, JAMA Netw. Open 2 (10) (2019), e1913619.

[4] J. Hu, L. Kong, J. Gao, W. Hu, X. Guan, J.J. Lu, Use of radiation therapy in metastatic nasopharyngeal cancer improves survival: a SEER analysis, Sci. Rep. 7 (1) (2017) 721.

[5] X.S. Sun, X.Y. Li, Q.Y. Chen, L.Q. Tang, H.Q. Mai, Future of radiotherapy in nasopharyngeal carcinoma, Br. J. Radiol. 92 (1102) (2019), 20190209.

[6] F.C. Ho, I.W. Tham, A. Earnest, K.M. Lee, J.J. Lu, Patterns of regional lymph node metastasis of nasopharyngeal carcinoma: a meta-analysis of clinical evidence, BMC Cancer 12 (2012) 98.

[7] G. Agarwal, P.J.B. Carcache, E.M. Addo, A.D. Kinghorn, Current status and contemporary approaches to the discovery of antitumor agents from higher plants, Biotechnol. Adv. 38 (2020), 107337.

[8] C.A.O.S., Editorial Committee of the Flora of China, Flora of China, Science Press, Beijing, 1977, pp. 416–434.

[9] D.H. Li, P. Hu, S.T. Xu, C.Y. Fang, S. Tang, X.Y. Wang, X.Y. Sun, H. Li, Y. Xu, X. K. Gu, J.Y. Xu, Lasiokaurin derivatives: synthesis, antimicrobial and antitumor biological evaluation, and apoptosis-inducing effects, Arch Pharm. Res. 40 (7) (2017) 796–806.

[10] H. Xing, L. An, Z. Song, S. Li, H. Wang, C. Wang, J. Zhang, M. Tuerhong, M. Abudukeremu, D. Li, D. Lee, J. Xu, N. Lall, Y. Guo, Anti-inflammatory *ent*-Kaurane Diterpenoids from Isodon Serra, J. Nat. Prod. 83 (10) (2020) 2844–2853.

[11] L. Ding, Q. Zhou, L. Wang, W. Wang, S. Zhang, B. Liu, Comparison of cytotoxicity and DNA damage potential induced by *ent*-Kaurene Diterpenoids from Isodon plant, Nat. Prod. Res. 25 (15) (2011) 1402–1411.

[12] E. Fujita, Y. Nagao, M. Node, K. Kaneko, S. Nakazawa, H. Kuroda, Antitumor activity of the isodon diterpenoids: structural requirements for the activity, Experientia 32 (2) (1976) 203–206.

[13] H.B. Zhang, J.X. Pu, Y.Y. Wang, F. He, Y. Zhao, X.N. Li, X. Luo, W.L. Xiao, Y. Li, H. D. Sun, Four new *ent*-Kauranoids from isodon rubescens var. lushanensis and data reassignment of dayecrystal B, Chem. Pharm Bull. 58 (1) (2010) 56–60.

[14] S. Nakamura, S. Sugimoto, T. Yoneda, A. Shinozaki, M. Yoshiji, T. Matsumoto, S. Nakashima, H. Matsuda, Antiproliferative activities of diterpenes from leaves of isodon trichocarpus against cancer stem cells, Chem. Pharm. Bull. 71 (7) (2023) 502–507.

[15] R. Liu, Z. Qu, Y. Lin, C.S. Lee, W.C. Tai, S. Chen, Brevilin a induces cell cycle arrest and apoptosis in nasopharyngeal carcinoma, Front Pharmacol. 10 (2019) 594.

[16] N.A. Franken, H.M. Rodermond, J. Stap, J. Haveman, C. van Bree, Clonogenic assay of cells *in vitro*, Nat. Protoc. 1 (5) (2006) 2315–2319.

[17] G. Chen, R. Gong, X. Shi, D. Yang, G. Zhang, A. Lu, J. Yue, Z. Bian, Halofuginone and artemisinin synergistically arrest cancer cells at the G1/G0 phase by upregulating $p21^{Cip1}$ and $p27^{Kip1}$, Oncotarget 7 (31) (2016) 50302–50314.

[18] R.H. Gong, D.J. Yang, H.Y. Kwan, A.P. Lyu, G.Q. Chen, Z.X. Bian, Cell death mechanisms induced by synergistic effects of halofuginone and artemisinin in colorectal cancer cells, Int. J. Med. Sci. 19 (1) (2022) 175–185.

[19] Z. Qu, Y. Lin, D.K. Mok, Q. Bian, W.C. Tai, S. Chen, Arnicolide D inhibits triple negative breast cancer cell proliferation by suppression of Akt/mTOR and STAT3 signaling pathways, Int. J. Med. Sci. 17 (11) (2020) 1482–1490.

[20] J. Marshall, Transwell((R)) invasion assays, Methods Mol. Biol. 769 (2011) 97–110.

[21] Y.M. Luo, S.D. Yang, M.Y. Wen, B. Wang, J.H. Liu, S.T. Li, Y.Y. Li, H. Cheng, L. L. Zhao, S.M. Li, J.J. Jiang, Insights into the mechanisms of triptolide nephrotoxicity through network pharmacology-based analysis and RNA-seq, Front. Plant Sci. 14 (2023), 1144583.

[22] W.N. Nik Nabil, Z. Xi, M. Liu, Y. Li, M. Yao, T. Liu, Q. Dong, H. Xu, Advances in therapeutic agents targeting quiescent cancer cells, Acta Mater. Med. 1 (1) (2022).

[23] C.M. Pfeffer, A.T.K. Singh, Apoptosis: a target for anticancer therapy, Int. J. Mol. Sci. 19 (2) (2018).

[24] I. Vermes, C. Haanen, H. Steffens-Nakken, C. Reutelingsperger, A novel assay for apoptosis. Flow cytometric detection of phosphatidylserine expression on early apoptotic cells using fluorescein labelled Annexin V, J. Immunol. Methods 184 (1) (1995) 39–51.

[25] J. Hasnan, M.I. Yusof, T.D. Damitri, A.R. Faridah, A.S. Adenan, T.H. Norbaini, Relationship between apoptotic markers (Bax and Bcl-2) and biochemical markers in type 2 diabetes mellitus, Singap. Med. J. 51 (1) (2010) 50–55.

[26] C. Gutta, A. Rahman, C. Aura, P. Dynoodt, E.M. Charles, E. Hirschenhahn, J. Joseph, J. Wouters, C. de Chaumont, M. Rafferty, M. Warren, J.J. van den Oord, W.M. Gallagher, M. Rehm, Low expression of pro-apoptotic proteins Bax, Bak and Smac indicates prolonged progression-free survival in chemotherapy-treated metastatic melanoma, Cell Death Dis. 11 (2) (2020) 124.

[27] W. Qu, S. Li, M. Zhang, Q. Qiao, Pattern and prognosis of distant metastases in nasopharyngeal carcinoma: a large-population retrospective analysis, Cancer Med. 9 (17) (2020) 6147–6158.

[28] Z. Su, Z. Yang, Y. Xu, Y. Chen, Q. Yu, Apoptosis, autophagy, necroptosis, and cancer metastasis, Mol. Cancer 14 (2015) 48.

[29] M. Yusuf, Y.A. Kusuma, D.R. Pawarti, Matrix metalloproteinase-9 expression and status of cervical lymph nodes in patients with nasopharyngeal carcinoma, Ind. J. Otolaryngol. Head Neck Surg. 71 (Suppl 1) (2019) 637–642.

[30] X. Fan, Y. Xie, H. Chen, X. Guo, Y. Ma, X. Pang, Y. Huang, F. He, S. Liu, Y. Yu, M. Hong, J. Xiao, X. Wan, M. Li, J. Zheng, Distant metastasis risk definition by tumor biomarkers integrated nomogram approach for locally advanced nasopharyngeal carcinoma, Cancer Control 26 (1) (2019), 1073274819883895.

[31] L.J.W. Pua, C.W. Mai, F.F. Chung, A.S. Khoo, C.O. Leong, W.M. Lim, L.W. Hii, Functional roles of JNK and p38 MAPK signaling in nasopharyngeal carcinoma, Int. J. Mol. Sci. 23 (3) (2022).

[32] Y. Kang, W. He, C. Ren, J. Qiao, Q. Guo, J. Hu, H. Xu, X. Jiang, L. Wang, Advances in targeted therapy mainly based on signal pathways for nasopharyngeal carcinoma, Signal Transduct. Target Ther. 5 (1) (2020) 245.

[33] N.V. Popova, M. Jucker, The role of mTOR signaling as a therapeutic target in cancer, Int. J. Mol. Sci. 22 (4) (2021).

[34] Y. Wang, J. Sun, N. Yao, Correlation of the AKT/mTOR signaling pathway with the clinicopathological features and prognosis of nasopharyngeal carcinoma, Eur. J. Histochem. 65 (4) (2021).

[35] Y. Si, J. Xu, L. Meng, Y. Wu, J. Qi, Role of STAT3 in the pathogenesis of nasopharyngeal carcinoma and its significance in anticancer therapy, Front Oncol. 12 (2022), 1021179.

[36] L.C. Kim, R.S. Cook, J. Chen, mTORC1 and mTORC2 in cancer and the tumor microenvironment, Oncogene 36 (16) (2017) 2191–2201.

[37] M. Jhanwar-Uniyal, J.V. Wainwright, A.L. Mohan, M.E. Tobias, R. Murali, C. D. Gandhi, M.H. Schmidt, Diverse signaling mechanisms of mTOR complexes: mTORC1 and mTORC2 in forming a formidable relationship, Adv. Biol. Regul. 72 (2019) 51–62.

[38] G.T. Chung, W.P. Lou, C. Chow, K.F. To, K.W. Choy, A.W. Leung, C.Y. Tong, J. W. Yuen, C.W. Ko, T.T. Yip, P. Busson, K.W. Lo, Constitutive activation of distinct NF-kappaB signals in EBV-associated nasopharyngeal carcinoma, J. Pathol. 231 (3) (2013) 311–322.

[39] J.T. Wee, T.C. Ha, S.L. Loong, C.N. Qian, Is nasopharyngeal cancer really a "Cantonese cancer"? Chin J. Cancer 29 (5) (2010) 517–526.

[40] P. Zhang, H. Hong, X. Sun, H. Jiang, S. Ma, S. Zhao, M. Zhang, Z. Wang, C. Jiang, H. Liu, MicroRNA-10b regulates epithelial-mesenchymal transition by modulating KLF4/Notch1/E-cadherin in cisplatin-resistant nasopharyngeal carcinoma cells, Am. J. Cancer Res. 6 (2) (2016) 141–156.

[41] L. Zhang, Q.Y. Chen, H. Liu, L.Q. Tang, H.Q. Mai, Emerging treatment options for nasopharyngeal carcinoma, Drug Des Devel. Ther. 7 (2013) 37–52.

[42] R. Liu, B. Dow Chan, D.K. Mok, C.S. Lee, W.C. Tai, S. Chen, Arnicolide D, from the herb centipeda minima, is a therapeutic candidate against nasopharyngeal carcinoma, Molecules 24 (10) (2019).

[43] J.P. Matson, J.G. Cook, Cell cycle proliferation decisions: the impact of single cell analyses, FEBS J. 284 (3) (2017) 362–375.

[44] Z.Y. Su, P.Y. Siak, C.O. Leong, S.C. Cheah, Nasopharyngeal carcinoma and its microenvironment: past, current, and future perspectives, Front Oncol. 12 (2022), 840467.